Available online at www.sciencedirect.com

jmr&t Journal of Materials Research and Technology

www.jmrt.com.br

Original Article

Comparative study of the pitting corrosion resistance, passivation behavior and metastable pitting activity of NO7718, NO7208 and 439L super alloys in chloride/sulphate media

Roland Tolulope Loto

Department of Mechanical Engineering, Covenant University, Ota, Ogun State, Nigeria

ARTICLE INFO

Article history:
Received 20 February 2018
Accepted 22 May 2018
Available online 22 June 2018

Keywords:
Corrosion
Pitting
Passivation
Alloy

ABSTRACT

Comparative study of the corrosion resistance and passivation characteristics of NO7718, NO7208 and SS439L super alloys in 4 M H_2SO_4 media at 0–6% NaCl concentration was done by potentiodynamic polarization, open circuit potential measurement and optical microscopic analysis. The metal alloys showed relatively high resistance to corrosion as variation in Cl^- ion concentration had no significant influence on their corrosion rate results. SS439L showed the weakest resistance to pitting despite its relatively low corrosion rate. Passivation behavior disappeared after 2% NaCl concentration. NO7208 displayed exceptional pitting resistance characteristics, however, its metastable pitting and repassivation domain responds to changes in Cl^- ion concentration. The passivation domain of NO7718 significantly decreased with increase in Cl^- ion concentration due to delayed repassivation of the protective film after metastable pitting. NaCl concentration caused significant negative shift in open circuit potential (OCP) for NO7718 and SS439L alloys, compared to NO7208. The OCP of NO7208 at comparatively positive values contrasts those of NO7718 and SS439L alloys. Micro analytical studies shows a highly corrosion resistant morphology for NO7208 with numerous macro-pits present but their effect on the overall corrosion resistance of the nickel alloy is negligible. The corrosion pits on SS439L coupled with the appearance of grain boundaries are deleterious to the overall viability of the alloy. Enlarged corrosion pits are present on NO7718 due to the action of Cl^- ions.

1. Introduction

Super alloys display excellent mechanical properties, surface stability, low corrosion susceptibility and high resistance to thermal deformation. This necessitates their extensive application as construction materials in nuclear industries, for piping and pumps in chemical processing and petrochemical industries, heat exchangers, in coal gasification and liquefaction systems, for the combustor and turbine

E-mail: tolu.loto@gmail.com
https://doi.org/10.1016/j.jmrt.2018.05.012

Table 1 – Nominal composition (wt.%) of N07718, N07208 and SS439L.

Element symbol	Cu	Si	Ni	Cr	Mn	P	S	C	Co	Al	Ti	Mo	N	Fe
% Composition (N07718)	0.3	0.35	51	18	0.35	0.04	0.05	0.08	0.8	0.3	1.1	3	–	24.72
% Composition (N07208)	–	0.15	56	20	0.3	–	–	0.06	10	1.5	2.1	8.5	–	1.5
% Composition (SS439L)	–	0.75	0.2	17.35	0.5	0.04	0.03	0.01	–		0.335	0.1	0.03	80.66

sections of the aero engine and land-based industrial-gas turbines, marine applications and pulp and paper manufacturing [1,2]. Their corrosion resistance is due primarily to the presence of chromium within their metallurgical structure, and responsible for the formation and stability of an impenetrable passive oxide film on the alloy surface when exposed to oxidizing conditions. The passive film hinders the electrochemical action of corrosive anions prevalent in industrial conditions due to their adherent inert nature. However there are circumstances where the passive film breaks due to a variety of causes in very hostile environments where high pressure and temperature conditions and strong halides are encountered. Collapse of the passive film and the consequent localized corrosion in the presence of chlorides is the major underlying factor responsible for failure of these alloys [3,4]. The electrochemical behavior of super alloys with respect to the formation, durability and breakdown of their passive film is integral to understanding of the metastable and pitting corrosion resistance of these alloys. In understanding the nature of passive film stability, potentiodynamic polarization and open circuit potential measurement are employed while the resulting microstructure from electrochemical study are further analyzed. Previous research on pit initiation and growth on stainless steel alloys have contributed to their current understanding and have help improve the pitting corrosion resistance of the alloys especially in the area of material selection and appropriate operating conditions [5–10]. Yi et al. [11] studied the pitting corrosion behavior of AISI type 316 SS in NaCl solutions by potentiodynamic polarization and concluded that its critical pitting potential is significantly influenced by the scan rate. Hodge and Wilde [12] observed through anodic polarization that Ni–Cr alloys with minimum 10% chromium become passive and displayed sufficient resistance to pitting in sulphate/chloride media. Piron et al. [13] observed similar behavior with Ni 200 and Inconel 600 in sulphate media at 0–3.5 wt.% NaCl. Breakdown of passivity on alloy 22 was observed by Friend [14] at a critical NaCl concentration by maintaining its potential inside the passive domain. The electrochemical behavior of alloy 600 and alloy 800 passive films was studied in various chemical environments [15,16]. Nickel chromium molybdenum alloys (NO7718 and NO7208) and ferritic stainless steel 439L exhibit excellent resistance to deterioration and failure in both oxidizing and reducing conditions. The ability of these alloys to withstand the effect corrosive anions is subject to the nature and constituent of their passive film, repassivation capacity, metastable pitting activity and pitting corrosion resistance. This research aims to study the passivation characteristics of the above-mentioned alloys in chloride/sulphate solutions and the resulting microstructure.

2. Experimental methods

NO7718 and NO7208 nickel alloys (NO7718, NO7208), and 439L ferritic stainless steel (SS439L) obtained from PCC Airfoils, LLC Prototype foundry, OH USA, Haynes International Incorporation, Kokomo, USA and McMaster University, Ontario, Canada are the super alloys studied. Their nominal (wt.%) compositions are laid out in Table 1. NO7718, NO7208 and SS439L were segmented and machined to samples with exposed surface areas of 0.4 cm^3, 0.4 cm^3 and 0.5 cm^3. They were subsequently prepared metallographically with the aid of silicon carbide abrasive papers of 60, 120, 220, 320, 600, 800 and 1000 grits before polishing with diamond liquid suspension to 6 μm, and then purified with distilled water and acetone for electrochemical tests. Recrystallized sodium chloride sourced from Titan Biotech, India was formulated in proportional concentrations of 0%, 1%, 2%, 3%, 4%, 5% and 6% in 200 mL of 4 M H_2SO_4 solution, prepared from standard grade of H_2SO_4 acid (98%) with distilled water.

Electrochemical tests were performed on the super alloys at 37 °C ambient temperature with a three electrodes cell (platinum counter electrodes, Ag/AgCl reference electrodes and resin embedded NO7718, NO7208 and SS439L electrodes) (exposed surface area of 1 cm^2) containing 200 mL of the acid media and connected to Digi-Ivy 2311 electrochemical workstation. Potentiodynamic polarization plots obtained at scan rate of 0.0015 V/s from −1.25 V and +1.5 V set potentials. The corrosion current density, C_d (A/cm^2) and corrosion potential, C_p (V) values were obtained from the polarization plots through Tafel extrapolation method. Corrosion rate, C_R (mm/y) and inhibition efficiency, η (%) were determined from the following mathematical relationship:

$$C_R = \frac{0.00327 C_d E_q}{D} \quad (1)$$

D is the density in (g/cm^3); E_q is the metal alloy equivalent weight (g). 0.00327 is the constant for corrosion rate. Open circuit potential measurement (OCP) was performed at 0.05 V/s step potential for 1500s to study the thermodynamic stability of the alloys at rest potentials. Micro-analytical images of the super alloys surface configuration were studied before and after electrochemical degradation with Omax trinocular metallurgical microscope using ToupCam analytical software.

3. Results and discussion

3.1. *Passivation studies*

The potentiodynamic polarization plots of NO7718, NO7208 and SS439L are shown from Fig. 1(a)–(c). Table 2 depicts

Table 2 – Potentiodynamic polarization data for NO7718, NO7208 and SS439L in 4 M H_2SO_4/0–6% NaCl concentration.

Sample	NaCl conc. (%)	Corrosion rate (mm/y)	Corrosion current (A)	Corrosion current density (A/cm^2)	Corrosion potential (V)	Polarization resistance, R_p (Ω)	Cathodic Tafel slope, B_c (V/dec)	Anodic Tafel slope, B_a (V/dec)
NO7718								
A	0	1.70	6.65E−05	1.62E−04	−0.025	386.10	−9.130	6.489
B	1	1.64	6.43E−05	1.57E−04	0.005	391.00	−10.780	26.670
C	2	1.57	6.17E−05	1.50E−04	−0.035	416.60	−10.850	21.200
D	3	1.59	6.22E−05	1.52E−04	−0.022	312.60	−12.430	21.270
E	4	1.44	5.65E−05	1.38E−04	−0.045	454.70	−9.915	20.500
F	5	1.39	5.45E−05	1.33E−04	−0.038	471.60	−11.600	22.700
G	6	1.63	6.38E−05	1.56E−04	−0.057	360.20	−11.390	27.610
NO7208								
A	0	0.49	1.93E−05	4.82E−05	−0.024	1334.00	−8.292	−1.978
B	1	0.48	1.85E−05	4.64E−05	−0.009	1985.00	−9.692	6.051
C	2	0.55	2.15E−05	5.37E−05	0.004	1197.00	−10.570	9.464
D	3	0.53	2.06E−05	5.14E−05	−0.006	1249.00	−10.800	8.225
E	4	0.50	1.97E−05	4.92E−05	−0.002	1300.00	−10.700	9.936
F	5	0.43	1.66E−05	4.15E−05	0.024	1549.00	−9.136	21.310
G	6	0.47	1.83E−05	4.57E−05	−0.064	1352.00	−9.362	8.645
SS439L								
A	0	0.09	5.07E−06	8.59E−06	0.083	5472.00	−14.000	8.525
B	1	0.07	4.12E−06	6.98E−06	−0.035	6242.00	−13.260	17.330
C	2	0.11	5.83E−06	9.88E−06	−0.066	5007.00	−9.379	21.010
D	3	0.07	3.76E−06	6.38E−06	−0.156	6829.00	−10.900	26.230
E	4	0.07	4.12E−06	6.98E−06	−0.197	6240.00	−9.002	15.810
F	5	0.09	5.19E−06	8.80E−06	−0.040	5171.00	−11.480	23.350
G	6	0.11	5.88E−06	9.97E−06	−0.082	5093.00	−9.435	10.850

the values of the polarization parameters obtained from the plots. The metal alloys showed relatively high resistance to corrosion. Variation in Cl^- ion concentration had no influence on their corrosion rate values, however, SS439L proves to be the most corrosion resistant followed by NO7208 from observation of corrosion rate values (Table 2). Passivity in metallic alloys emanates from the presence of hydrated Cr_2O_3 within the passive film. The passivation behavior of the metal alloys contrasts the corrosion rate values due to differential changes in their film composition to a more oxidized form in the presence of chlorides. The high reactivity of Cl^- ions is due to their small size, mobility, high dispersion solubility [17]. Under high potential difference Cl^- ions diffuse through the protective film displacing H_2O and OH groups and inducing the localized breakdown of the passive layer. NO7208 maintained a stable passivation domain at all Cl^- ion concentration studied (1–6% NaCl). The potential at which pitting occurred on the alloy tends to be relatively stable signifying strong pitting corrosion resistance. Its passive film being highly resistive, pitting most probably do take place at sites where there are flaws, inclusions or defects. However, the metastable pitting and repassivation domain of NO7208 responds to changes in Cl^- concentration (Fig. 1(b)) resulting in extended anodic polarization plot due to short term dissolution, visible metastable pitting activity and decreased passivation domain. The passivation domain of NO7718 significantly decreased with increase in Cl^- ion concentration due to delayed repassivation of the protective film after metastable pitting. Shortening of the passive domain was accompanied by sufficient increase in corrosion current density. This is

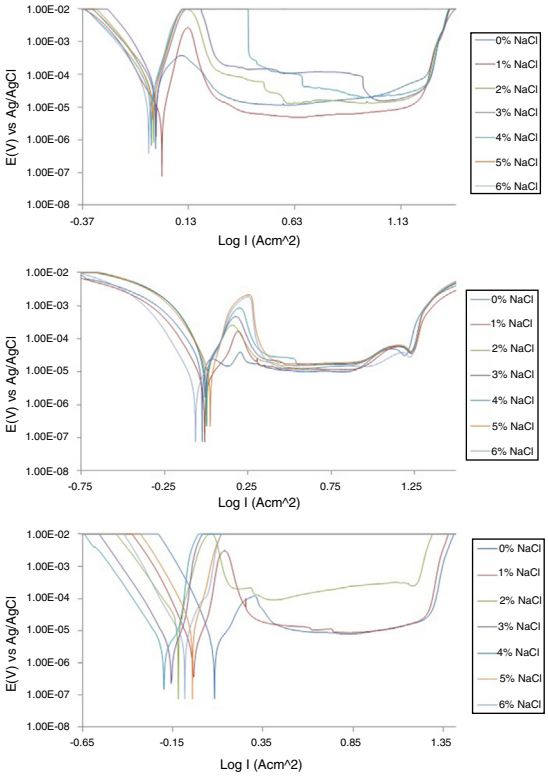

Fig. 1 – Polarization plots of (a) NO7718 alloy (b) NO7208 alloy and (c) SS439L alloy in 4 M H_2SO_4/0–6% NaCl concentration.

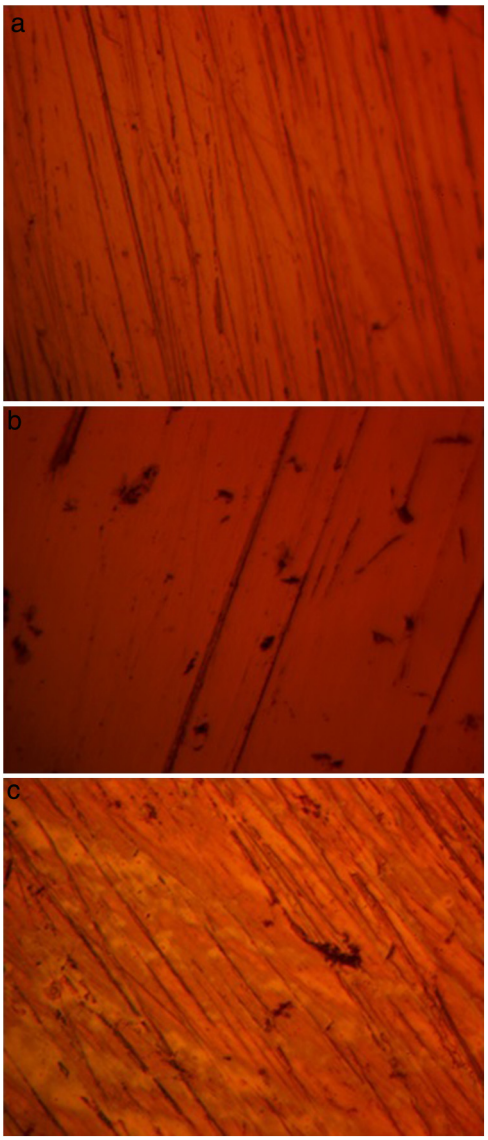

Fig. 2 – Micro-analytical images of (a) NO7718, (b) NO7208 and (c) SS439L at mag. 100× before corrosion.

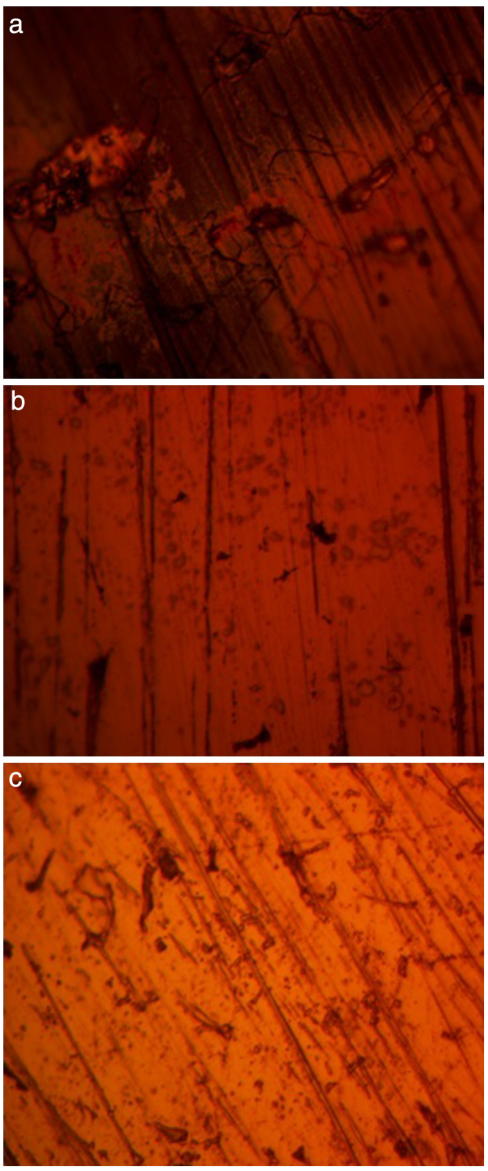

Fig. 3 – Micro-analytical images of (a) NO7718, (b) NO7208 and (c) SS439L at mag. 100× after corrosion in 4 M H_2SO_4/0% NaCl.

characteristic to dissolution of the passive film in addition to initiation of localized corrosion. Beyond 4% NaCl concentration passivation behavior was completely absent on NO7718 polarization plot due to the debilitating action of Cl^- ions. The increase in Cl^- ion concentration caused instability the passive films eventually resulting in breakdown as confirmed through micro analytical observations to be discussed later. The potential domain for passivation reduced, and formation of the protective stopped due to dominant electro-dissolution reaction processes. SS439L metal alloy showed the weakest resistance to pitting corrosion despite its relatively low corrosion rate. Passivation behavior disappeared after 2% NaCl concentration as a result of the inability of the protective film to reform after anodic polarization. The low Cl^- ion concentrations were not adequate to impair the passive film and initiate pitting on SS439L and NO7718 metal alloys. At higher Cl^- ion concentrations, the passive film breakdown exceeded film formation resulting in the formation of stable corrosion pits. The exceptional pitting resistance property of NO7208 is ascribed to the coaction of Cr and Mo [18,19]. Mo causes the passive film to be more stable against localized breakdown resulting from the Cl^- ions and promotes the repassivation characteristics.

3.2. *Microanalytical studies*

Fig. 2(a) and (b) shows the optical microscopic morphology of NO7718, NO7208 and SS439L metal alloys before corrosion test with visible metallurgical flaws present on NO7208 and SS439L morphology. The morphology of the alloys after corrosion in 4 M H_2SO_4/0% NaCl (Fig. 3(a) and (b)) slightly contrast the images in Fig. 2(a) and (b). A dark superficial inert oxide is visible on NO7718 (Fig. 3(a)) coupled with an etched worn out morphology due to the electrochemical action of SO_4^{2-} ions. Numerous macro-pits are present on NO7208

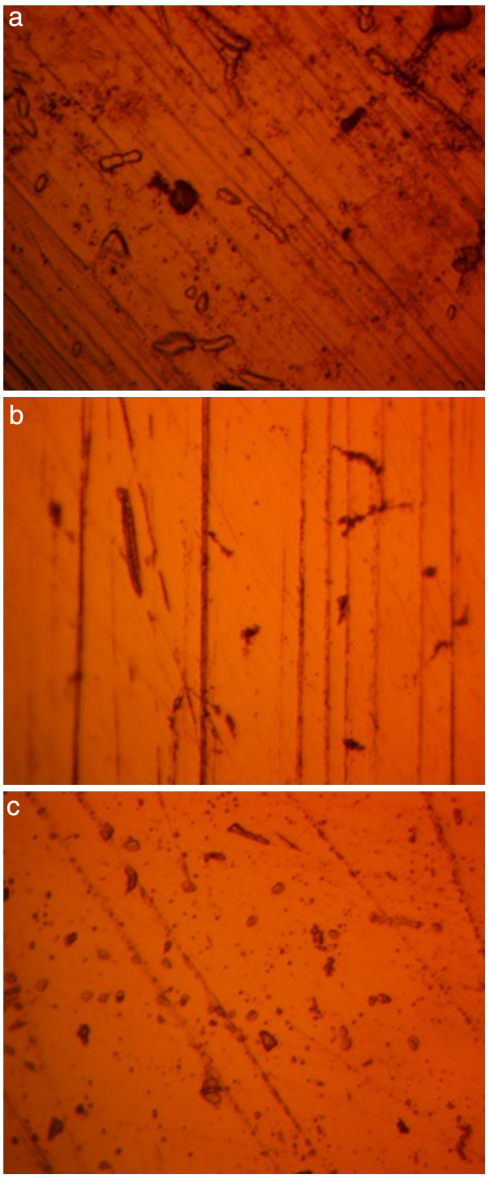

Fig. 4 – Micro-analytical images of (a) NO7718, (b) NO7208 and (c) SS439L at mag. 100× after corrosion in 4 M H_2SO_4/1% NaCl.

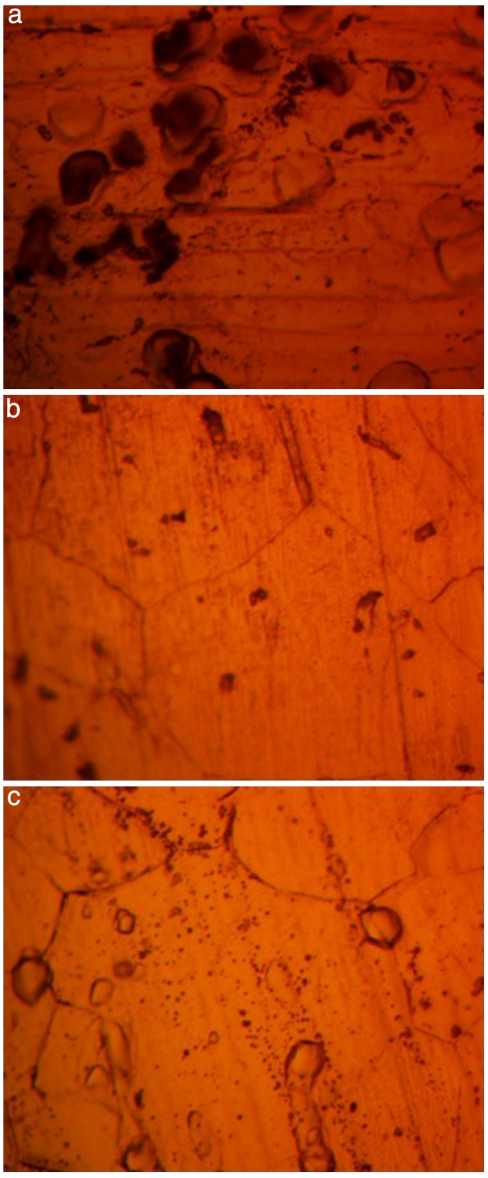

Fig. 5 – Micro-analytical images of (a) NO7718, (b) NO7208 and (c) SS439L at mag. 100× after corrosion in 4 M H_2SO_4/6% NaCl.

morphology, but their effect on the overall corrosion resistance of the nickel alloy is negligible. The protective film on the nickel alloy is basically Ni–Cr–Fe oxide. The high Cr content of the oxides accounts in large part for the high corrosion resistance of these alloys. Micro-pits are present on SS439L whose uncertain depths are most likely deleterious to the overall viability of the alloy with respect to results from polarization test. Increase in Cl^- ion concentration to 1% NaCl further deteriorates the morphology of the metal alloys (Fig. 4(a)–(c)) with visible formations of macro/micro-pits associated with pitting corrosion. The visible corrosion susceptibility is attributed to the dissolution of their passive film constituents. After corrosion in 4 M H_2SO_4/6% NaCl (Fig. 5(a)–(c)), the corrosion pits on NO7718 (Fig. 5(a)) has enlarged due to increased action of Cl^- ions. Anodic dissolution of the alloy surfaces (Fig. 5(a)–(c)) are visible with grain boundaries gradually appearing on SS439L alloy.

3.3. *Open circuit potential measurement*

Thermodynamic stability of passive oxide films constituents strongly influences the corrosion resistance of metal alloys and it gives suitable insight into the active passive behavior of the films without applied potential. The open circuit potential (OCP) measured against exposure time for NO7718, NO7208 and SS439L metal alloys in 4 M H_2SO_4/0%, 1% and 6% NaCl concentration is shown in Fig. 6(a)–(c). The presence of NaCl in the acid media caused significant negative shift in OCP value for NO7718 and SS439L alloys, compared to NO7208 most especially at 6% NaCl signifying dominant cathodic corrosion

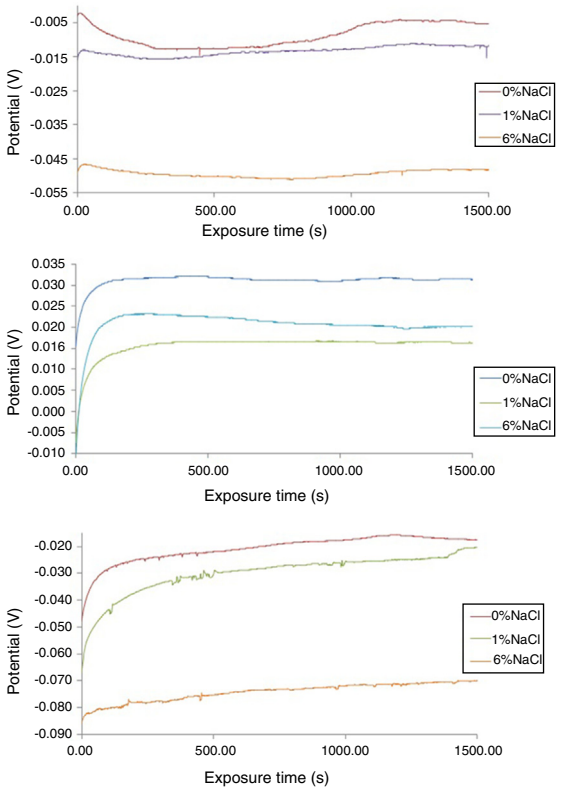

Fig. 6 – OCP curves of corrosion potential versus exposure time for (a) NO77189, (c) NO7208 and SS439L in 4 M H_2SO_4/0–6% NaCl.

reaction processes for both alloys with respect to Cl^- ion concentration. The positive increase in potential for SS439L at 0%, 1% and 6% NaCl signifies the time dependent gradual formation of a protective passive film at the alloy surface. Potential transients are visible on the curves for SS439L at 1% and 6% NaCl due to active-passive behavior of the alloy related to the breakdown and repassivation of the protective film. The decrease in potential for NO7718 (0% NaCl) to $-0.012\,V_{Ag/AgCl}$ at 260.1 s is due to cathodic polarization behavior related to interfacial degradation of the alloy. The alloy remained at this equilibrium till 700.01 s at $-0.013\,V_{Ag/AgCl}$ before potential increase to $-0.005\,V_{Ag/AgCl}$ at 1075.36 s due to passivation of the alloy. Slightly similar phenomenon occurred for NO7718 at 6% NaCl, however, the presence of Cl^- ions delayed the formation of the passive film on the alloy. The OCP of NO7208 (0%, 1% and 6% NaCl concentration) at values comparatively positive in contrast to NO7718 and SS439L alloys is due generally to the higher corrosion resistance displayed by NO7208 throughout the exposure hours. Increase in potential of NO7208 curves continued for the first 300 s after which the OCP curve at 0% and 1% NaCl relatively stabilized due to the stability and strength of the protective film formed on NO7208 surface. However, a gradual but mild time dependent increase in potential was observed for NO7208 OCP curve at 6% NaCl before stabilizing at $0.021\,V_{Ag/AgCl}$ (1000.01 s) after the first initial 300 s due to crack/heal event during which sufficient hydrated chromium oxyhydroxide was formed and sustained.

4. Conclusion

NO7208 proves to be highly resistant to pitting corrosion in acid chloride media due to the stability of its film at all chloride concentrations studied from optical microscopic images. However, it undergoes significant anodic dissolution resulting from metastable pitting and delayed repassivation of the protective film with respect to chloride concentration. The nickel alloy showed thermodynamic stability at positive potentials with minimal shift in OCP values. NO7208 and SS439L undergoes significant pitting corrosion with increase in chloride concentration resulting in loss of passivity at 4% and 2% NaCl. Significant shift in their OCP values occurred in the presence of chlorides at negative potentials due to cathodic polarization. Optical images confirmed the presence of corrosion pits on the metal alloys.

Conflicts of interest

The authors declare no conflicts of interest.

REFERENCES

[1] Caron P, Khan T. Evolution of Ni-base superalloys for single crystal gas turbine blade applications. Aerosp Sci Technol 1999;3:513–23.
[2] Hashizume R, Yoshinari A, Kiyono T, Murata Y, Morinaga M. Development of Ni-based single crystal superalloys for power generation gas turbines. Mater Sci Eng Energy Syst 2007;2(1):5–12.
[3] McCafferty E. Sequence of steps in the pitting of aluminum by chloride ions. Corros Sci 2003;45:1421–38.
[4] Abdel Rehim SS, Hassan HH, Amin MA. Chronoamperometric studies of pitting corrosion of Al and (Al–Si) alloys by halide ions in neutral sulphate solutions. Corros Sci 2004;46:1921–38.
[5] Loto RT, Loto CA. Potentiodynamic polarization behavior and pitting corrosion analysis of 2101 duplex and 301 austenitic stainless steel in sulfuric acid concentrations. J Fail Anal Prev 2017;17(4):672–9.
[6] Loto RT, Loto CA. Pitting corrosion inhibition of type 304 austenitic stainless steel by 2 amino 5 ethyl 1,3,4 thiadiazole in dilute sulphuric acid. Prot Metals Phys Chem Surf 2015;51(4):693–700.
[7] Loto RT. Pitting corrosion evaluation of austenitic stainless steel type 304 in acid chloride media. J Mater Environ Sci 2013;4(4):448–59.
[8] Tian W, Du N, Li S, Chen S, Wu Q. Metastable pitting corrosion of 304 stainless steel in 3.5% NaCl solution. Corros Sci 2014;85:372–9.
[9] Orlikowski J, Jazdzewska A, Mazur R, Darowicki K. Determination of pitting corrosion stage of stainless steel by galvanodynamic impedance spectroscopy. Electrochim Act 2017;253:403–12.
[10] Ha H-Y, Lee T-H, Kim S-J. Synergistic effect of Ni and N on improvement of pitting corrosion resistance of high nitrogen stainless steels. Corros Eng Sci Techn 2013;49(2):82–6.
[11] Yi Y, Cho P, Al Zaabi A, Addad Y, Jang C. Potentiodynamic polarization behaviour of AISI type 316 stainless steel in NaCl solution. Corros Sci 2013;74:92–7.

[12] Hodge FG, Wilde BE. Effect of chloride ion on the anodic dissolution kinetics of chromium–nickel binary alloys in dilute sulfuric acid. NACE Corros 1970;26(6):246–50.
[13] Piron DL, Koutsoukos EP, Nobe K. Corrosion behavior of nickel and inconel in acidic chloride solutions. NACE Corros 1969;25(4):151–6.
[14] Friend WZ. Nickel–chromium-molybdenum alloys. New York: Wiley-Interscience; 1980.
[15] Ming-Yu C, Ge-Ping Y. Pitting corrosion of inconel 600 in chloride and sulfate solutions at low temperature. J Nucl Mater 1993;202(1–2):145–53.
[16] Zeqing W, Jianqiu W, Yashar B, Zhiming G, Jihui W, Da-Hai X. Pitting growth rate on Alloy 800 in chloride solutions containing thiosulphate: image analysis assessment. Corros Eng Sci Techn 2018;53(3):206–13.
[17] Ibrahim MAM, Abd El Rehim SS, Hamza MM. Corrosion behavior of some austenitic stainless steels in chloride environments. Mater Chem Phys 2009;115:80–5.
[18] Thiago JM, Eric C, Marc M, Nicole K, Ricardo PN. Influence of Mo alloying on pitting corrosion of stainless steels used as concrete reinforcement. Rem: Rev Esc Minas 2013;66(2):173–8.
[19] Qvarfort R. Some observations regarding the influence of molybdenum on the pitting corrosion resistance of stainless steels. Corros Sci 1998;4(2–3):215–23.